A Study on the Control of an IPMC Actuator Using an Adaptive Fuzzy Algorithm

Sin-Jong Oh, Hunmo Kim*
School of Mechanical Engineering, Sungkyunkwan University, Chunchun-dong Jangan-Gu Suwon 440-746, Korea

The Ionic Polymer Metal Composite (IPMC) is one of the electroactive polymers (EAP) that was shown to have potential application as an actuator. It bends by applying a low voltage current (1~3 V) to its surfaces when containing water. In this paper, the basic characteristics and the static & dynamic modeling of IPMC is discussed. In modeling and analysis, the equations of motion, which describe the total dynamics of the system, are driven. To control the position of the IPMC actuator, an adaptive fuzzy algorithm is used. IPMC is a time varying system because the some parameters vary with the passage of time. In this paper, the modeling and control of IPMC is introduced.

Key Words: IPMC, EAP, Adaptive Fuzzy Algorithm, FMRLC

1. Introduction

Research on EAP applications has progressed over the last few years. IPMC among various EAPs have many advantages. IPMC can be driven at low voltage (1~3volt), can be miniaturized easily, and is made of flexible material. Therefore, many studies about the possibility of utilization are under way. For example, IPMC was applied to an active catheter system (Guo et al., 1995), a distributed actuation device (Tadokoro et al., 1998), an underwater robot (Guo et al., 1998), a micropump (Guo et al., 1999), micro manipulators (Tadokoro et al., 1999), a face-type actuator (Tadokoro et al., 1999), and a wiper of an asteroid rover (Bar-Cohen et al., 2000). IPMC was especially utilized in the endoscopic microcapsule studied by the author together with electrostrictive polymer (EP) (Kornbluh et al., 2000; Zhenyl et al., 1994; Heydt et al., 1998), because it is good for the human body.

We will develop the cilium of a micro endoscope, which can play a role in shifting directions. Fig. 1 shows the IPMC cilium of a micro endoscope. The dimension of a saw-toothed IPMC is 2.5 mm×2 mm×0.2 mm in Fig. 1. As the saw-toothed IPMC located at the end of an actuator bends backward and forward, the system changes directions. To apply IPMC to many actuators, a system model must be established. Ordinary industrial products are designed using models and CAE, by which design efficiency becomes much higher than the methodology as a result of experiments, and trial and error. It is really difficult in a practical sense to use mechanisms and materials that do not have appropriate models for CAE, even if they have many

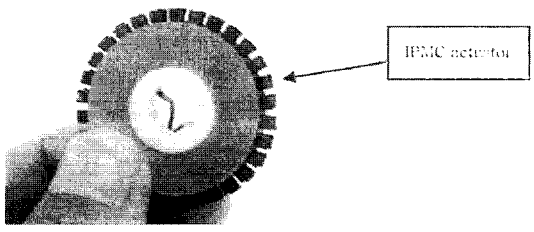

Fig. 1 IPMC actuator

* Corresponding Author,
E-mail: kimhm@me.skku.ac.kr
TEL: +82-31-290-7450; **FAX**: +82-31-290-5849
School of Mechanical Engineering, Sungkyunkwan University, Chunchun-dong Jangan-Gu Suwon 440-746, Korea. (Manuscript **Received** July 15, 2002; **Revised** July 28, 2003)

advantages. Up till now mathematical modeling has closely studied by a few researchers.(Kanno et al., 1996 ; Tadokoro et al., 2000a, 2000b) But the general characteristics and the non-linearity of IPMC have not been carried out accurately. In this paper, the static modeling of the IPMC is performed through some experiments.

The relations between voltage and displacement are derived from experimentation. The dynamic modeling based on the static modeling of the IPMC is performed using Lagrange's equation, but this model is not enough to express the nonlinearity of the IPMC actuator because it is not completely developed in terms of the inner physical characteristics of IPMC. Also, this model is assumed to be the time invariant system with time constant parameters. A fuzzy control algorithm is only suitable for simulation, so finally the controller consists of an adaptive fuzzy algorithm with reference model. It is for this reason that we need a way to automatically tune the fuzzy controller so that it can adapt to different plant conditions.

2. General Characteristics of IPMC

2.1 Principle of operation

The general IPMC is composed of a perfluorinated ion exchange membrane, which is chemically plated with a metal such as gold (Yoshiko et al., 1998) or platinum. The typical chemical structure of a polymer is

$$[-(CF_2\text{-}CF_2)_n\text{-}(CF\text{-}CF_2)\text{-}]_m$$
$$\qquad\qquad\qquad\qquad\qquad\quad |$$
$$\qquad\qquad\qquad\qquad O\text{-}CF\text{-}CF_2\text{-}O\text{-}CF_2\text{-}SO_3^-\ldots\ldots M^+$$
$$\qquad\qquad\qquad\qquad\quad\ |$$
$$\qquad\qquad\qquad\qquad\quad CF_3$$

where n~6.5, 100<m<1000, and M+ is the counter ion (H+, Li+ or Na+). The mechanism for electrical actuation is considered due to electro-osmotic pressure (Okade et al., 1998). When a certain voltage is applied to a normal electrolyte, cations and anions that migrate in opposite directions with there being both ion-dipole interaction and momentum transfer can carry no net momentum transfer to the solvent. In Nafion, the SO_3^- group is fixed to the matrix while the counter-ion (cation) is free to move. When voltage is applied to the hydrated sample, the counter-ion will migrate to the cathode and simultaneously push water to this side. As a result, IPMC swells and expands at the cathode. A concentration gradient in water will be induced and back-diffusion may be responsible for the observed relaxation of the membrane. It has measured the water transference coefficient for a variety of cations in Nafion.

2.2 Distinguished characteristics

IPMC have the following characteristics that are distinguished from actuators

- The driving voltage is low (1.0~2.5V)
- Its response frequency is high (>100 Hz)
- It is a soft material ($E=2.2\times10^8$ Pa)
- Miniaturization is possible (<1 mm)
- Durability is high ($>1\times10^6$ bending cycles)
- The force generated is small, so excessive force cannot be applied (0.8 g_f at the tip of a cantilever-shaped actuator (5 mm×25 mm×0.2 mm)) at 3 V
- It moves when it contains water (in a wet condition).
- It is not a force-type actuator, but a position-type actuator.
- Its distributed actuator function realizes actuation with multiple degrees of freedom.

3. Static Modeling

3.1 Basic experiment

In the meantime, there has been a lot of work phenomena, in which bending motion phenomenon appears when electric force is supplied. Although a relative equation was derived through analyzing the driving principle of IPMC mechanical, electrical, and chemical aspects, all the properties of the IPMC were not expressed. (Kanno et al., 1994) System Identification (SI) is accomplished by input and output values before deriving the general equation inside the material in this paper.

Fig. 2 shows the experimental setup for measurement of displacement and force. Fig. 3 shows

(a)

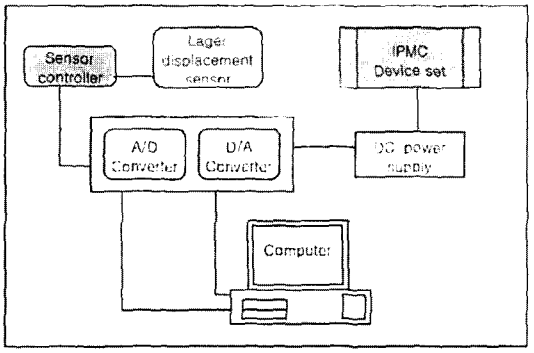

(b)

Fig. 2 (a) The measurement device set for displacement and force of IPMC (b) Experimental setup

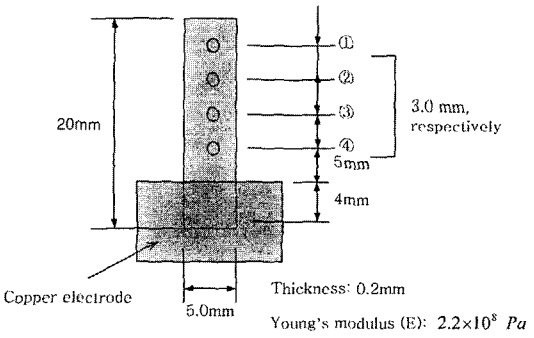

Fig. 3 IPMC (5 mm×20 mm×0.2 mm) between copper electrodes for experiment

IPMC specimen (5 mm×20 mm×0.2 mm) double coated with platinum fixed between copper electrodes for the experiment. After each point (①, ②, ③, ④) of the specimen is marked with a white pen, its displacement for change of input voltage is measured using a laser displacement sensor.

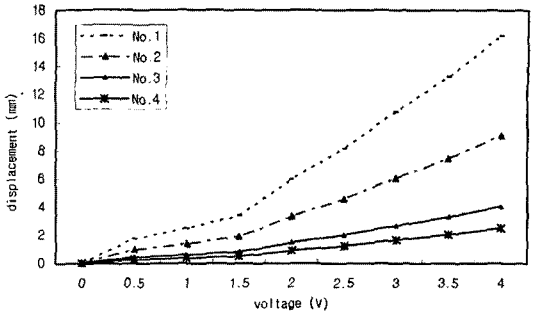

(a)

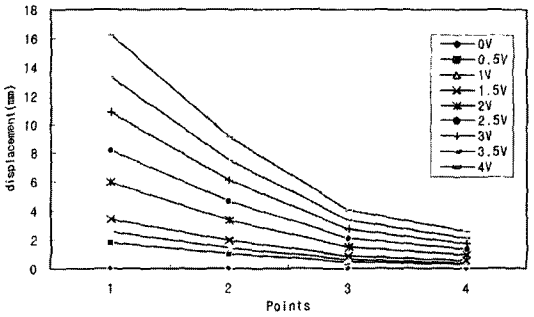

(b)

Fig. 4 Displacement of each point of IPMC with respect to input voltage

Displacement values at each point in the IPMC as in Fig. 4, when various input voltages (1.5 Hz frequency) are supplied. If a point is far from the copper electrode, displacement is larger. In other words, it has been discovered that the bending of an edge of IPMC is the largest.

3.2 Relation between force and displacement

This experiment is repeated as the voltage changes, and the equation expressing the relation between supplied voltage and maximum deflection (displacement), (1) is derived.

$$\delta_{max}=\frac{9.4}{125}\times L \times(-0.0016V(t)^5+0.691V(t)^3+0.611V(t)) \quad (1)$$

The relation between a force and displacement is obtained from Fig 4.

$$EI\cdot W(x)=\frac{P_0}{120L}(L-x)^5-\frac{P_0}{24}L^3(L-x)+\frac{P_0}{30}L^4 \quad (2)$$

By substituting δ_{max} in (1) into $W(x)$ in (2), P_0 is obtained as

$$P_0=\frac{30EI}{L^4}\cdot\delta_{max} \tag{3}$$

Using (3), the assumed force applied IPMC is derived as

$$\begin{aligned}P(x)&=-\frac{P_0}{L}(x-L)\\&=-\frac{30EI}{L^5}\cdot\delta_{max}(x-L)\end{aligned} \tag{4}$$

4. Dynamic Modeling

4.1 Assumption

IPMC is a time varying system because the parameters involved in its dynamic equations, such as a density and Young's modulus, vary with time. IPMC works normally in a wet condition as previously stated. Fig. 5 shows the variation of the water content of IPMC with respect to time. Equation (5) is based on this result.

$$\rho(t)=2.44\times10^{-3}\cdot(0.857+0.143\cdot e^{-0.00035t}) \tag{5}$$

Young's modulus is also derived from the water content and equation is represent as (Grot et al., 1972)

$$E/E_0=\exp\left[-\alpha\left(c+\frac{1200-M_{eq}}{20}\right)\right] \tag{6}$$

$E_0=0.275$ GPa, $\alpha=0.294$,
$c=$ *grams of water per* 100 g *of dry polymer*
$M_{eq}=1100$ *for Nafion* 117

Equation (6) is transformed into time equation as follows:

$$\begin{aligned}E(t)=&0.275\cdot e^{-0.0294\times(16.67\cdot e^{-0.00035t}+5)}\\&\times10^9(\mathrm{g/mm^2})\end{aligned} \tag{7}$$

From (6) and (7) new variable, $H(t)$ is obtained as:

$$\begin{aligned}H(t)&=\frac{E(t)}{\rho(t)}\\&=\frac{0.275\cdot e^{-0.0294\times(16.67\cdot e^{-0.00035t}+5)}\times10^9(\mathrm{g/mm^2})}{2.44\times10^{-3}\cdot(0.857+0.143\cdot e^{-0.00035t})}\end{aligned} \tag{8}$$

Fig. 6 shows the equation $H(t)$. Equation (8) is linearized as follows:

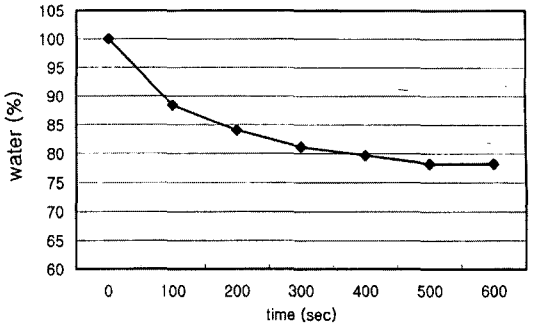

Fig. 5 The rate of water with respect to time

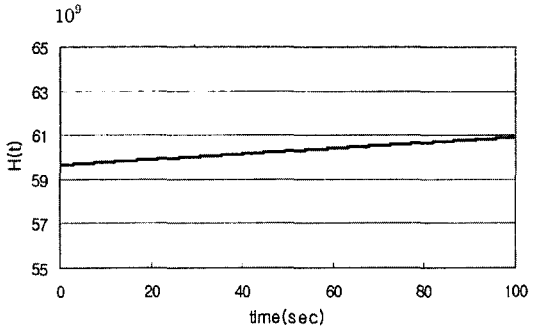

Fig. 6 Linear approximate of $E(t)/\rho(t)$ with respect time

$$H(t)=(0.0128t+59.637)\times10^9 \tag{9}$$

In this paper, the gradient of $H(t)$ is regarded as zero in a short period. And it is assumed that the water is supplied during IPMC actuation. And because density and Young's modulus hardly change over a short time, density and Young's IPMC modulus is regarded as constant and the system is time invariant as a result.

4.2 Equations of motion

Fig. 7 shows the simplified model considered in this study. To obtain the equations of motion, Lagrange's equation (Robert 1998) is used. From Fig. 7, the kinetic energy, T and the potential energy, V are represented, respectively as

$$T=\frac{1}{2}\int_0^L\rho A\dot{W}^2dx \tag{10}$$

$$V=\frac{1}{2}\int_0^L EI(W'')^2dx \tag{11}$$

where ρ is the mass per unit length, A is the cross section and EI is the flexural rigidity of the beam.

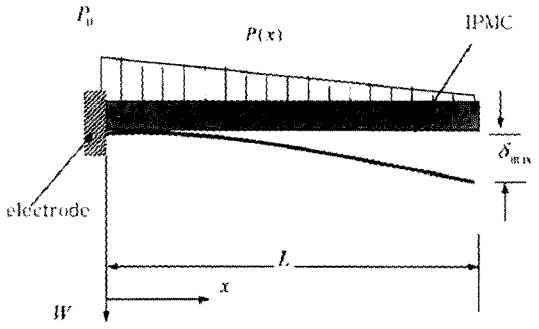

Fig. 7 Simplified model of IPMC as applying an input voltage

Because the IPMC is assumed to be the cantilever beam, the boundary conditions are represented as:

$$W(0, t)=0,\ W'(0, t)=0,\\ W''(0, t)=0,\ W'''(0, t)=0 \tag{12}$$

Integration of (11) by parts leads to:

$$\begin{aligned} V&=\frac{1}{2}\int_0^L EI\left[\frac{\partial^2 W(x, t)}{\partial x^2}\right]^2 dx\\ &=\left[\left|\frac{\partial W(x, t)}{\partial x}\cdot\frac{\partial^2 W(x, t)}{\partial x^2}\right|_0^L\right.\\ &\quad-\left|W(x, t)\cdot\frac{\partial^3 W(x, t)}{\partial x^3}\right|_0^L\\ &\quad\left.+\int_0^L W(x, t)\cdot\frac{\partial^4 W(x, t)}{\partial x^4}dx\right]\cdot\frac{1}{2}EI \end{aligned} \tag{13}$$

Substitution of (12) into (13) results in the following:

$$V=\int_0^L W(x, t)\cdot\frac{\partial^4 W(x, t)}{\partial x^4}dx \tag{14}$$

From (10) and (14)

$$\begin{aligned} L=T-V&=\frac{1}{2}\int_0^L \rho A\dot{W}^2 dx\\ &\quad-\frac{1}{2}EI\int_0^L W(x, t)\cdot\frac{\partial^4 W(x, t)}{\partial x^4}dx \end{aligned} \tag{15}$$

where L is a Lagrangian function. To obtain the equations of motion, the Lagrange' equation is used as follows:

$$\frac{d}{dt}\left(\frac{\partial L}{\partial \dot{W}}\right)-\frac{\partial L}{\partial W}=P(x) \tag{16}$$

By substituting (15) into (16), equations of IPMC are derived as:

$$\rho A\ddot{W}+EI\cdot\frac{\partial^4 W(x, t)}{\partial x^4}=P(x) \tag{17}$$

4.3 Modal analysis

4.3.1 Homogeneous solution

In (17), by letting $P(x)=0$, the following equation is obtained:

$$C^2\cdot\frac{\partial^4 W(x, t)}{\partial x^4}+\frac{\partial^2 W(x, t)}{\partial t^2}=0 \tag{18}$$

where $c=\sqrt{\dfrac{EI}{\rho A}}$

To solve the partial differential equation in (18), taking the separation of variables as:

$$W(x, t)=X(x)\cdot T(t) \tag{19}$$

where deflection, $W(x, t)$ is assumed to be related to the function including only x and t respectively. Substitution of (19) into (18) results in:

$$\frac{c^2}{X(x)}\cdot\frac{d^4X(x)}{dx^4}=-\frac{1}{T(t)}\cdot\frac{d^2T(t)}{dt^2}=\omega^2 \tag{20}$$

Equation (20) can be decomposed into two equations as:

$$\frac{d^4X(t)}{dx^4}-\beta^4X(x)=0,\ \beta^4=\frac{\omega^2}{c^2} \tag{21}$$

$$\frac{d^2T(t)}{dt^2}+\omega^2\cdot T(t)=0 \tag{22}$$

where (21) represents the mode shape and (22) determines the modal amplitude. Solving the differential equation of (21) leads to:

$$X_n(x)=[(\cosh\beta_n x-\cos\beta_n x)-\sigma_n(\sinh\beta_n x-\sin\beta_n)] \tag{23}$$

where

$$\sigma_n=\frac{\sinh\beta_n L-\sin\beta_n L}{\cosh\beta_n L+\cos\beta_n L} \tag{24}$$

including the modal damping term, $2\xi\omega\cdot\dot{T}(t)$ with the modal equation, (22) results in:

$$\frac{d^2T(x)}{dt^2}+2\xi\omega\cdot\frac{dT(t)}{dt}+\omega^2\cdot T(t)=0 \tag{25}$$

Solving (25), the modal amplitude, $T_n(t)$ is obtained as:

$$T_n(t)=e^{-\xi_n\omega_n t}\{c_0\cos(\omega_n\sqrt{1-\xi_n^2}\cdot t)+c_1\sin(\omega_n\sqrt{1-\xi_n^2}\cdot t)\} \tag{26}$$

By substituting (23) and (26) into (19), the homogeneous solution, $W_h(x, t)$ is obtained as:

$$W_h(x,t)=\sum_{n=1}^{\infty}X_n(x)\cdot T_n(t)$$
$$=\sum_{n=1}^{\infty}[(\cosh\beta_n x-\cos\beta_n x)-\sigma_n(\sinh\beta_n x-\sin\beta_n x)] \quad (27)$$
$$\times e^{-\xi_n\omega_n t}\{c_0\cos(\omega_n\sqrt{1-\xi_n^2}\cdot t)+c_1\sin(\omega_n\sqrt{1-\xi_n^2}\cdot t)\}$$

4.3.2 Particular solution

Equation (17) is not solved by the separation of variables because of the $P(x)$ term. So the deflection, $W(x, t)$ is assumed to have a solution of the form:

$$W(x,t)=M(x,t)+\phi(x) \quad (28)$$

The substitution of (28) into (17) leads to:

$$\rho A\ddot{M}+EI\cdot\frac{\partial^4 M(x,t)}{\partial x^4}+\frac{\partial^4\phi(x)}{\partial x^4}=P(x) \quad (29)$$

$$\frac{\partial^4\phi(x)}{\partial x^4}-P(x)=0 \quad (30)$$

If the chosen $\phi(x)$ satisfies (30), the boundary conditions in (12) are described as

$$\begin{aligned}&W(0,t)=M(0,t)+\phi(0)=0\\&W'(0,t)=M'(0,t)+\phi'(0)=0\\&W''(L,t)=M''(L,t)+\phi''(L)=0\\&W'''(L,t)=M'''(L,t)+\phi'''(L)=0\end{aligned} \quad (31)$$

where, if $\phi(0)=\phi'(0)=\phi''(L)=\phi'''(L)=0$, (31) is simply rewritten as:

$$\begin{aligned}&W(0,t)=M(0,t)=0\\&W'(0,t)=M'(0,t)=0\\&W''(L,t)=M''(L,t)=0\\&W'''(L,t)=M'''(L,t)=0\end{aligned} \quad (32)$$

Substitution of (4) into (30) offers:

$$\frac{\partial^4\phi(x)}{\partial x^4}=-\frac{30EI}{L^5}\cdot\delta_{\max}(x-L) \quad (33)$$

Solving the differential equation, $\phi(x)$ is obtained as:

$$\phi(x)=EI\cdot\delta_{\max}\left(-\frac{x^5}{4L^5}+\frac{5x^4}{4L^4}-\frac{5x^3}{2L^3}+\frac{5x^2}{2L^2}\right) \quad (34)$$

If the initial velocity and displacement of IPMC is zero, there is $W(x, 0)=\dot{W}(x, 0)=0$ Equation (28) is represented as:

$$\begin{aligned}&M(x,0)=W(x,0)-\phi(x)=-\phi(x)\\&\dot{M}(x,0)=\dot{W}(x,0)=0\end{aligned} \quad (35)$$

In (27) $W(x, t)$ is displaced with $M(x, t)$ as:

$$M(x,t)=\sum_{n=1}^{\infty}[(\cosh\beta_n x-\cos\beta_n x)-\sigma_n(\sinh\beta_n x-\sin\beta_n x)] \quad (36)$$
$$\times e^{-\xi\omega_n t}\{c_0\cos(\omega_n\sqrt{1-\xi^2}\cdot t)+c_1\sin(\omega_n\sqrt{1-\xi^2}\cdot t)\}$$

By substituting $t=0$ into (36), it is rewritten as:

$$M(x,0)=\sum_{n=1}^{\infty}[(\cosh\beta_n x-\cos\beta_n x)-\sigma_n(\sinh\beta_n x-\sin\beta_n x)]\times c_0$$
$$=-EI\cdot\delta_{\max}\left(-\frac{x^5}{4L^5}+\frac{5x^4}{4L^4}-\frac{5x^3}{2L^3}+\frac{5x^2}{2L^2}\right) \quad (37)$$

To solve (37), the orthogonality is used as follows:

$$\int_0^L[(\cosh\beta_n x-\cos\beta_n x)-\sigma_n(\sinh\beta_n x-\sin\beta_n x)]\cdot M(x,0)\cdot dx$$
$$=c_0\times\int_0^L[(\cosh\beta_n x-\cos\beta_n x)-\sigma_n(\sinh\beta_n x-\sin\beta_n x)]^2dx \quad (38)$$

Solving $\dot{M}(x, 0)$ by the same methods, c_0 and c_1 are obtained as:

$$c_0=\frac{1}{Q_n(x)}\int_0^L X_n(x)\cdot M(x,0)\cdot dx \quad (39)$$

$$c_1=\frac{1}{Q_n(x)}\int_0^L X_n(x)\cdot\dot{M}(x,0)\cdot dx \quad (40)$$

where

$$Q(x)=\int_0^L[(\cosh\beta_n x-\cos\beta_n x)-\sigma_n(\sinh\beta_n x-\sin\beta_n x)]^2dx \quad (41)$$

From (35) $c_1=0$. And c_0 is rewritten as:

$$c_0=\frac{1}{Q_n(x)}\times\int_0^L\cdot-EI\cdot\delta_{\max}\left(-\frac{x^5}{4L^5}+\frac{5x^4}{4L^4}-\frac{5x^3}{2L^3}+\frac{5x^2}{2L^2}\right)X_n(x)\cdot dx$$
$$=\frac{S_n(x)}{Q_n(x)} \quad (42)$$

where

$$S_n(x)=\int_0^L\cdot-EI\cdot\delta_{\max}\left(-\frac{x^5}{4L^5}+\frac{5x^4}{4L^4}-\frac{5x^3}{2L^3}+\frac{5x^2}{2L^2}\right)X_n(x)\cdot dx \quad (43)$$

From (36) and (42), $M(x, t)$ is rewritten as:

$$M(x,t)=\sum_{n=1}^{\infty}[(\cosh\beta_n x-\cos\beta_n x)-\sigma_n(\sinh\beta_n x-\sin\beta_n x)] \quad (44)$$
$$\times[c_0\cdot e^{-\xi\omega_n t}\cos(\omega_n\sqrt{1-\xi^2}\cdot t)]$$

From (28), (34) and (44), the deflection, $W(x, t)$ is obtained finally as:

$$W(x,t)=\sum_{n=1}^{\infty}[(\cosh\beta_n x-\cos\beta_n x)-\sigma_n(\sinh\beta_n x-\sin\beta_n x)] \times\{c_0\cdot e^{-\xi\omega_n t}\cos(\omega_n\sqrt{1-\xi^2}\cdot t)] +EI\cdot S_{\max}\left(-\frac{x^5}{4L^5}+\frac{5x^4}{4L^4}-\frac{5x^3}{2L^3}+\frac{5x^2}{2L^2}\right) \quad (45)$$

5. Adaptive Fuzzy Controller

5.1 Fuzzy model reference learning control (FMRLC)

A control is necessary for shifting the direction of the IPMC actuator. If the common PID control method is used as the position control of an IPMC actuator, it is difficult to obtain accuracy. Because the system modeling derived in the previous section provides some assumptions and uncertainties.

Meanwhile fuzzy logic generally does not require a perfectly precise system model in the design of the controller. (Mamdani, 1974; Yager and Filev, 1994) Also, a fuzzy control design method can be easily applied via human expert's knowledge (through many experiments) based on a dynamic system established in advance. Because the design process for fuzzy controllers that is based on the use of heuristic information from human experts has found success in many industrial applications. In this paper, an adaptive fuzzy controller is used. It is for this reason that we need a way to automatically tune the fuzzy controller so that it can adapt to different plant conditions (density and Young's modulus in here). Fig. 8 shows the diagram of FMRLC. It has four main parts: the plant, the fuzzy controller to be tuned, the reference model, and the learning mechanism (an adaptation mechanism). A reference model is used with a mathematical model in Chapter. 4.

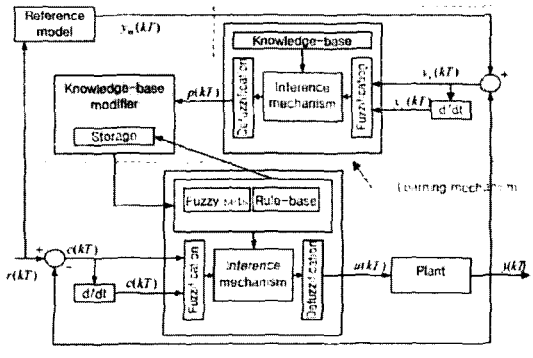

Fig. 8 Fuzzy model reference learning controller (FMRLC)

To make a fuzzy controller, control inputs are defined as an error (e) and a change in error (c) as follows:

$$e(kT)=r(kT)-y(kT)$$
$$c(kT)=\frac{e(kT)-e(kT-T)}{T} \quad (46)$$

T=*sampling time*
$r(kT)$=*reference input*
$y(kT)$=*measurement input*

And control output (u) is defined as input voltage to actuate the IPMC.

For easy computation, the membership functions of the linguistic terms for each input variable is represented to the triangular shape functions (see Fig. 9). Seven linguistic terms: NB (negative big), NM (negative medium), NS (negative small), ZE (zero), PS (positive small), PM (positive medium), and PB (positive big) are defined for input fuzzy variables, as shown in

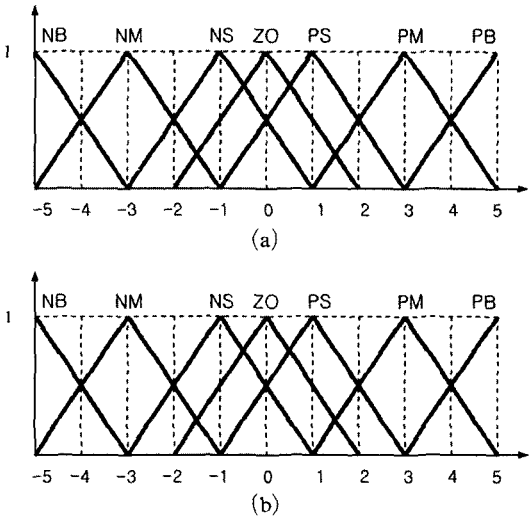

Fig. 9 (a) Membership functions of error and change in error (b) change in output (for fuzzy model)

Table 1 Membership function

	NB	NM	NS	ZO	PS	PM	PB
−5	**1.0**	0.0	0.0	0.0	0.0	0.0	0.0
−4	**0.5**	**0.5**	0.0	0.0	0.0	0.0	0.0
−3	0.0	**1.0**	0.0	0.0	0.0	0.0	0.0
−2	0.0	**0.5**	**0.5**	0.0	0.0	0.0	0.0
−1	0.0	0.0	**1.0**	**0.5**	0.0	0.0	0.0
0	0.0	0.0	**0.5**	**1.0**	**0.5**	0.0	0.0
1	0.0	0.0	0.0	**0.5**	**1.0**	0.0	0.0
2	0.0	0.0	0.0	0.0	**0.5**	0.0	0.0
3	0.0	0.0	0.0	0.0	0.0	**1.0**	0.0
4	0.0	0.0	0.0	0.0	0.0	**0.5**	**0.5**
5	0.0	0.0	0.0	0.0	0.0	0.0	**1.0**

Table 2 Rule base for fuzzy controller

e \ c	NB	NM	NS	ZO	PS	PM	PB
NB	0	0	NM	NB	NM	0	0
NM	0	0	NS	NM	NS	0	0
NS	0	0	ZO	NS	ZO	0	PM
ZO	NB	NM	NS	ZO	PS	PM	PB
PS	NM	0	ZO	PS	ZO	0	0
PM	0	0	PS	PM	PS	0	0
PB	0	0	PM	PB	PM	0	0

Table 1. A rule-based table for output variables of the fuzzy logic control system is shown in Table 2.

The rule base is determined throughout the characteristic experiments of the IPMC. It is composed of the form of 'If-THEN' as :

$$IF\ \tilde{e}\ is\ \tilde{E}\ and\ \tilde{c}\ is\ \tilde{C}\ THEN\ \tilde{u}\ is\ \tilde{U} \quad (47)$$

Fuzzification performs a mapping from a scaled crisp input value and the Mamdani method (Robert, 1998 ; Mamdani, 1974) is used for fuzzy inference :

$$\mu_r(e, c, u) = Min(\mu_E(e), \mu_C(c), \mu_U(u))$$
$$\mu_{U'}(u) = Max - Min(\mu_E(e'), \mu_C(c'), \mu_U(u')) \quad (48)$$

5.2 Learning mechanism

The learning mechanism tunes the rule-base of the direct fuzzy controller so that the closed loop system behaves like the reference model. These

Table 3 Fuzzy rule base fuzzy inverse model

e \ c	NB	NS	ZO	PS	PB
NB	0	NM	NB	NM	0
NS	0	ZO	NS	ZO	PM
ZO	NB	NS	ZO	PS	PB
PS	NM	ZO	PS	ZO	0
PB	0	PM	PB	PM	0

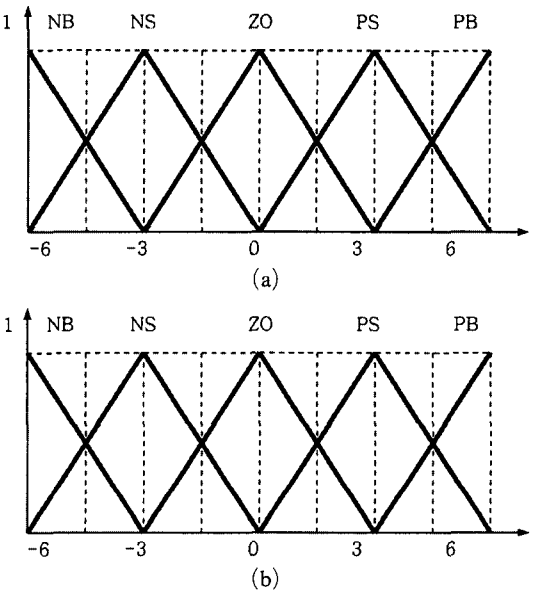

Fig. 10 (a) Membership functions of error and change in error (b) Membership function of change in output (for fuzzy inverse model)

rule-base modifications are made by observing data from the controlled process, the reference model, and the fuzzy controller. This rule-base is described in Table 3. and membership function for fuzzy inverse model is depicted in Fig. 10. The learning mechanism consists of two parts : a 'fuzzy inverse model (Tsoukalas and Uhrig, 1997)' and a 'knowledge-base modifier'.

The rule-base for the fuzzy inverse model contains rules of the form :

$$IF\ \tilde{y}_e\ is\ Y_e^j\ and\ \tilde{y}_c\ is\ Y_c^l\ THEN\ \tilde{p}\ is\ P^m \quad (49)$$

where Y_e^j and Y_c^l denote linguistic values an d $\tilde{P}^m$ denotes the linguistic value associated with the m^{th} output fuzzy set. y_e and y_c is represented as follows :

$$y_e(kT)=y_m(kT)-y(kT)$$
$$y_c(kT)=\frac{y_e(kT)-y_e(kT-T)}{T} \quad (50)$$
$$y_m(kT)=\textit{reference model output}$$

Let $b_m(kT)$ denote the center of the m^{th} output membership function at time kT. For all rules in the active set, use

$$b_m(kT)=b_m(kT-T)+p(kT) \quad (51)$$

to modify the output membership function centers.

6. Results

6.1 Simulation

To verify the dynamic modeling of the IPMC actuator performed in Chapter 4, computer simulation is executed.

Fig. 11 shows the displacement of the end point of the IPMC (20 mm×5 mm×0.2 mm) according to the time when various voltages are applied. Fig. 12 shows the displacement of the whole length of IPMC as time changes (0.5 sec, 1 sec, 2 sec, 3 sec) when the same voltage (2 volt) is applied.

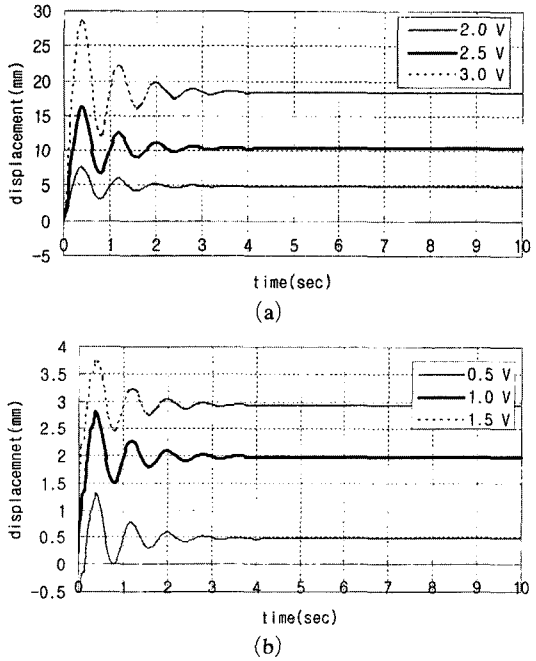

Fig. 11 Simulation result of IPMC (Displacements of the end point of IPMC at different step input voltages)

We find that the displacement is the largest at the early stage (0.5 sec). After some oscillations are generated the end point of IPMC fixes any displacement in Fig. 12.

Fig. 13 shows the result of the fuzzy controller versus no control.

6.2 Experimentation

The actuator was set up in a cantilever configuration from a set of electrodes. The tip displacement was measured by a laser sensor LK-081. Voltage to the IPMC was applied through an AD/DA board containing a DC-power supply. An adaptive fuzzy algorithm is coded by C-language.

Fig. 14 shows the experimental measurement of the end point of the IPMC for step inputs. The measurement result between 0.3 sec and 0.55 sec is not obtained because the laser sensor cannot

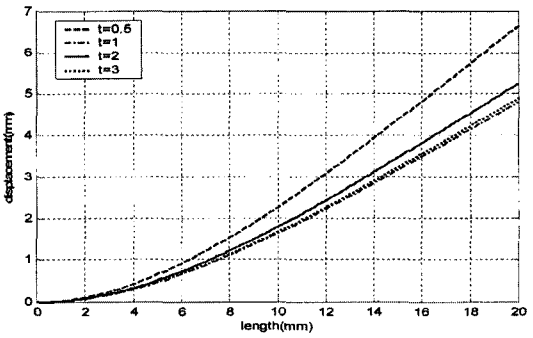

Fig. 12 Simulation result of IPMC (Displacements of IPMC with respect to constant time @ 2.0 volt)

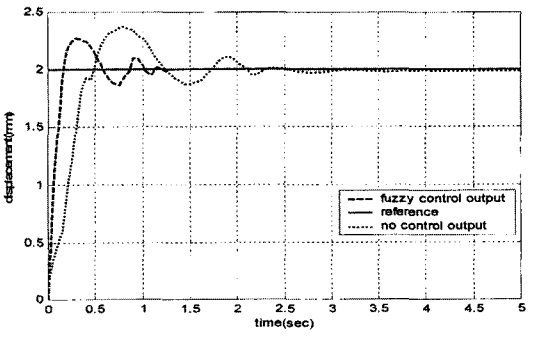

Fig. 13 Simulation control for fuzzy controller

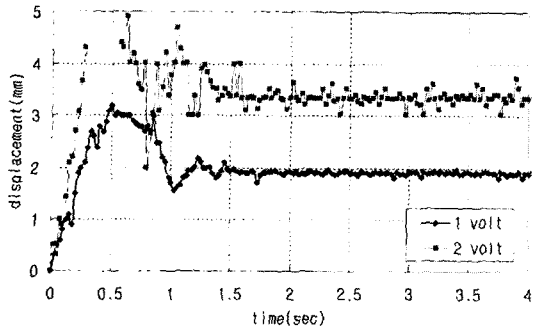

Fig. 14 Experimental measurement of the end point of the IPMC for step inputs

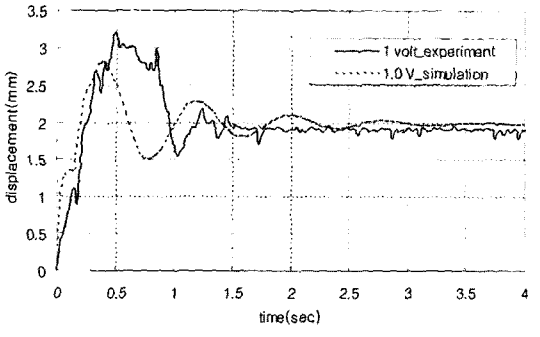

Fig. 15 Comparison of the results of Experiment and simulation at 1 Volt (step input)

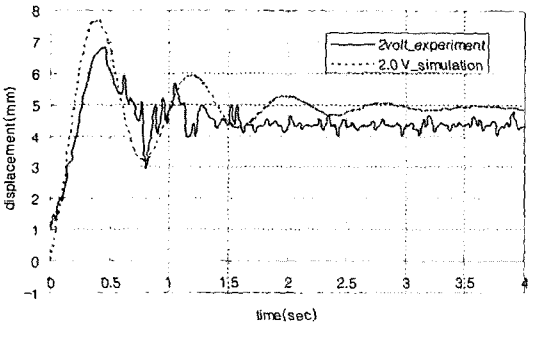

Fig. 16 Comparison of the results of Experiment and simulation at 2 Volt (step input)

detect the value in the case of pronounced bending of the IPMC. Fig. 14 also shows that it is the more difficult to maintain a fixed position at high voltage. Fig. 15 and Fig. 16 show the comparison of simulation and experimental result.

Figure 17 shows the adaptive fuzzy control result. The result of an adaptive fuzzy control shows that a faster settling time and smaller overshoot compared with the others. Also, the oscillations decrease at a steady state.

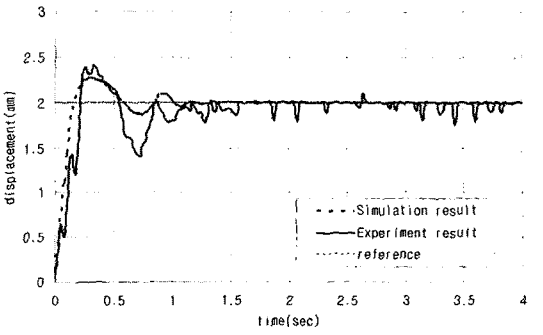

Fig. 17 Control response

7. Conclusion

To control the IPMC actuator, the following study was performed :

(1) The relation of voltage and maximum displacement was derived from the basic experiment of the IPMC.

(2) The static model of a strip type was fined as a base of experimental expression.

(3) The dynamic modeling was based on the static model, derived by using the Lagrange's equation.

(4) The computer simulation verified the modeling results.

(5) An adaptive fuzzy algorithm was used for position control of the IPMC actuator. And differences between simulations and experimental measurement are shown.

This paper has shown that adaptive fuzzy control in IPMC, and the control algorithm was suitable for controlling IPMC.

Acknowledgment

This work was performed under the management of the Intelligent Micro Center at 21C Frontier R&D Program sponsored by Korea Ministry of Science and Technology.

References

Bar-Cohen, Y., Leary, S., Yavrouian, A., Oguro, K., Tadokoro, S., Harrison, J., Smith, J.

and Su, J., 2000, "Challenge to the Application of IPMC as Actuators of Planetary Mechanism," In: *Smart Structures and Materials* (Y. Bar-Cohen, Ed.). Proc. SPIE Vol. 3987, pp. 140~146, Newport Beach, USA.

Grot, W. G. F., Munn, C. E. and Walmsly, P. N. 1972, 141st Meeting of the Electrochemical Society, Houston, Texas, May 1972, Abstract No. 154; *J. Electrochem. Sco.*, 119, 108C.

Guo, G. et al., 1995, "Micro Catheter System with Active Guide Wire," Proc. IEEE ICRA, pp. 79~84.

Guo, G. et al., 1998, "Development of Underwater Micro Robot Using ICPF Actuator," Proc. IEEE ICRA, pp. 1829~1835.

Guo, G. et al., 1999, "Development of a New Type of Capsule Micropump," Proc. IEEE ICRA, pp. 2171~2176.

Heydt, R., Kornbluh, R., Pelrine, R. and Mason, V., 1998, "Design and Performance of an Electrostrictive-Polymer-Film Acoustic Actuator," J. Sound and vibration, Vol. 215, No. 2, pp. 297~311.

Kanno, R. et al., 1996, "Linear Approximate Dynamic Model of an ICPF (Ionic Conducting Polymer Gel Film) Actuator," Proc. IEEE ICRA, pp. 219~225.

Kanno, R. et al., 1994, "Characteristics and modeling of ICPF actuator," *Proc. JUSFA*, pp. 692~698.

Kornbluh, R., Ronald Pelrine, Qibing Pei, Seajin Oh, and Jose Joseph, 2000, "Ultrahigh Strain Response of Field-Actuated Elastomeric Polymers," In: *Smart Structures and Materials* (Bar-Cohen, Y., Ed.), Proc. SPIE Vol. 3987, pp. 51~64, Newport Beach, USA.

Mamdani, E. H., 1974, "Application of Fuzzy Algorithm for Control of Simple Dynamic Systems," in *Proc. Inst. Elect. Eng.*, Vol. 121, No. 12, pp. 1585~1588.

Okade, T., Xie, G., Gorseth, O. et al., 1998, "Ion and Water Transport Characteristics of Nafion Membranes as Electrolytes," *Electrochem. Acta*, Vol. 43, No. 24, pp. 3741~3747.

Robert E. Skelton, 1998, "Dynamic Systems Control: Linear Systems Analysis and Synthesis," John Whily & Sons, Inc, New York.

Tadokoro, S. et al., 1998, "Development of a Distributed Actuation Device Consisting of Soft Gel Actuator Elements," Proc. IEEE ICRA, pp. 2155~2160.

Tadokoro, S. et al., 1999, "Development of a Multi-Degree of Freedom Micro Motion Device Consisting of Soft Gel Actuators," J. Robotics and Mechatronics.

Tadokoro, S. et al., 1999, "Distributed Actuation Devices Using Soft Gel Actuators," Distributed Manipulation, Kluwer Academic.

Tadokoro, S., Shinji Yamagami, Toshi Takamori and Keisuke Oguro., 2000a, "Modeling of Nafion- Pt composite actuators (ICPF) by ionic motion," In: *Smart Structures and Materials* (Y. Bar-Cohen, Ed.), Proc. SPIE Vol. 3987, pp. 92~109, Newport Beach, USA.

Tadokoro, S., Masahiko Fukuhara, Y. Bar-Cohen, Keisuke Oguro, Toshi Takamori, 2000b, "A CAE Approach in Application of Nafion-Pt Composite (ICPF) Actuators-Analysis for Surface Wipers of NASA MUSES-CN Nanorovers," In: *Smart Structures and Materials* (Y. Bar-Cohen, Ed.), Proc. SPIE Vol. 3987, pp. 262~272, Newport Beach, USA.

Tsoukalas, L. H. and Uhrig, R. E., 1997, *Fuzzy and Neural Approaches in Engineering*. New York: Wiley.

Yager, R. R. and Filev, D. P., 1994, *Essentials of Fuzzy Modeling and Control*. New York: Wiley.

Yoshiko, A., Mochizuki, A., Kawashima, T., Tamashita, S., Asaka, K. and Oguro, K., 1998, "Effect on Bending Behavior of Counter Cation Species in Perfluorinated Sulfonate Membrance-Platinum Composite," *Polymer for Advanced Technologies*, Vol. 9, pp. 520~526.

Zhenyl, M, J. I., Scheinbeim, J. W., Lee, and B. A. Newman, 1994, "High Field Electrostrictive Response of Polymers," Journal of Polymer Sciences, Part B-Polymer Physics, Vol. 32, pp. 2721~2731.